Environ. Chem. **2016**, *13*, 723–731
doi:10.1071/EN14247_AC ©CSIRO 2016

Supplementary material

Arsinothricin, a novel organoarsenic species produced by a rice rhizosphere bacterium

Masato Kuramata,[A] *Futa Sakakibara,*[B,D] *Ryota Kataoka,*[B,E] *Kenichi Yamazaki,*[B] *Koji Baba,*[B] *Masumi Ishizaka,*[B] *Syuntaro Hiradate,*[C] *Tsunashi Kamo*[C] *and Satoru Ishikawa*[A,F]

[A]Soil Environment Division, National Institute for Agro-Environmental Sciences,
3-1-3 Kannondai, Tsukuba, Ibaraki 305-8604, Japan.

[B]Organochemical Division, National Institute for Agro-Environmental Sciences,
3-1-3 Kannondai, Tsukuba, Ibaraki 305-8604, Japan.

[C]Biodiversity Division, National Institute for Agro-Environmental Sciences,
3-1-3 Kannondai, Tsukuba, Ibaraki 305-8604, Japan.

[D]Department of Applied Biology and Chemistry, Tokyo University of Agriculture,
1-1-1 Sakuragaoka, Setagaya-ku, Tokyo 156-8502, Japan.

[E]Faculty of Life and Environmental Sciences, University of Yamanashi,
4-4-37 Takeda, Koufu, Yamanashi 400-8510, Japan.

[F]Corresponding author. Email: isatoru@affrc.go.jp

©CSIRO 2016

Table S1. Parameters for the UPLC-MS-MS analysis

Q-Exactive (Thermo Fisher Scientific)		Micromass Quattro Micro API (Waters)	
LC conditions		UPLC conditions	
Column	Waters Atlantis dC18 3 µm (2.1-mm ID × 100 mm)	Column	Waters Acquity UPLC BEH C18 1.7 µm (2.1-mm ID × 100 mm)
Mobile phase	10 % (v/v) CH_3CN, 10 mM NH_4OAc (pH 5.5)	Mobile phase	0.1 % (v/v) HCOOH; 10 mM NH_4OAc (pH 5.5)
Flow rate	0.1 mL min^{-1}	Flow rate	0.2 mL min^{-1}
Injection volume	2 µL	Injection volume	10 µL
Column temperature	40 °C	Column temperature	40 °C
MS conditions		MS conditions	
Ionisation mode	Electrospray ionisation	Ionisation mode	Electrospray ionisation
Capillary voltage	3.5 kV	Capillary voltage	3.5 kV
Vaporiser temperature	300–350 °C	Desolvation temperature	350 °C
Capillary temperature	250 °C	Source temperature	120 °C
N_2 gas flow rate (arbitrary units)	45/10	Cone gas flow rate (L h^{-1})	50
S-lens level	50	RF lens	0.2 V
MS detection		MS detection	
Scan range	*m*/*z* 65.00–600.00	Scan range	*m*/*z* 50–250
MS-MS detection		MS-MS detection	
Normalised collision energy	35 % (HCD) stepped 40 %	Collision energy	13.0–14.0 V
Scan range	*m*/*z* 50.00–485.00	Scan range	*m*/*z* 50–250

©CSIRO 2016

Table S2. Column recoveries of As species in the samples

Values are rearranged data from Fig. 2. The recovery value represents the sum of the As species relative to the initial 13.3 μM As^{III} concentration

Culture period	Concentration (μM)				Recovery (%)
(h)	Inorganic As	AST	AST-OH	Sum	
5	14.5	0.0	0.0	14.5	108.8
9	14.3	0.0	0.0	14.3	106.9
15	14.7	0.0	0.0	14.7	110.6
24	14.2	0.0	0.5	14.7	110.0
36	13.4	0.0	1.1	14.5	108.9
48	12.7	0.4	1.7	14.8	110.6
60	11.9	0.7	1.9	14.5	108.8
72	11.1	1.3	1.8	14.2	106.5
84	10.7	1.7	1.8	14.2	106.0
96	10.4	2.1	1.8	14.3	106.8
120	10.4	2.3	1.7	14.4	108.2

Table S3. ^{1}H NMR (600 MHz) and ^{13}C NMR (150 MHz) spectral data for arsinothricin (AST) recorded in D_2O

Position	δ_H (ppm)	δ_C (ppm)
C-1	–	173.9
C-2	3.84 (1H, t, *J* 5.7 Hz)	55.4
C-3	2.42 (2H, m)	29.6
C-4	2.26 (2H, m)	22.9
C-5	1.97 (3H, s)	16.5

 ©CSIRO 2016

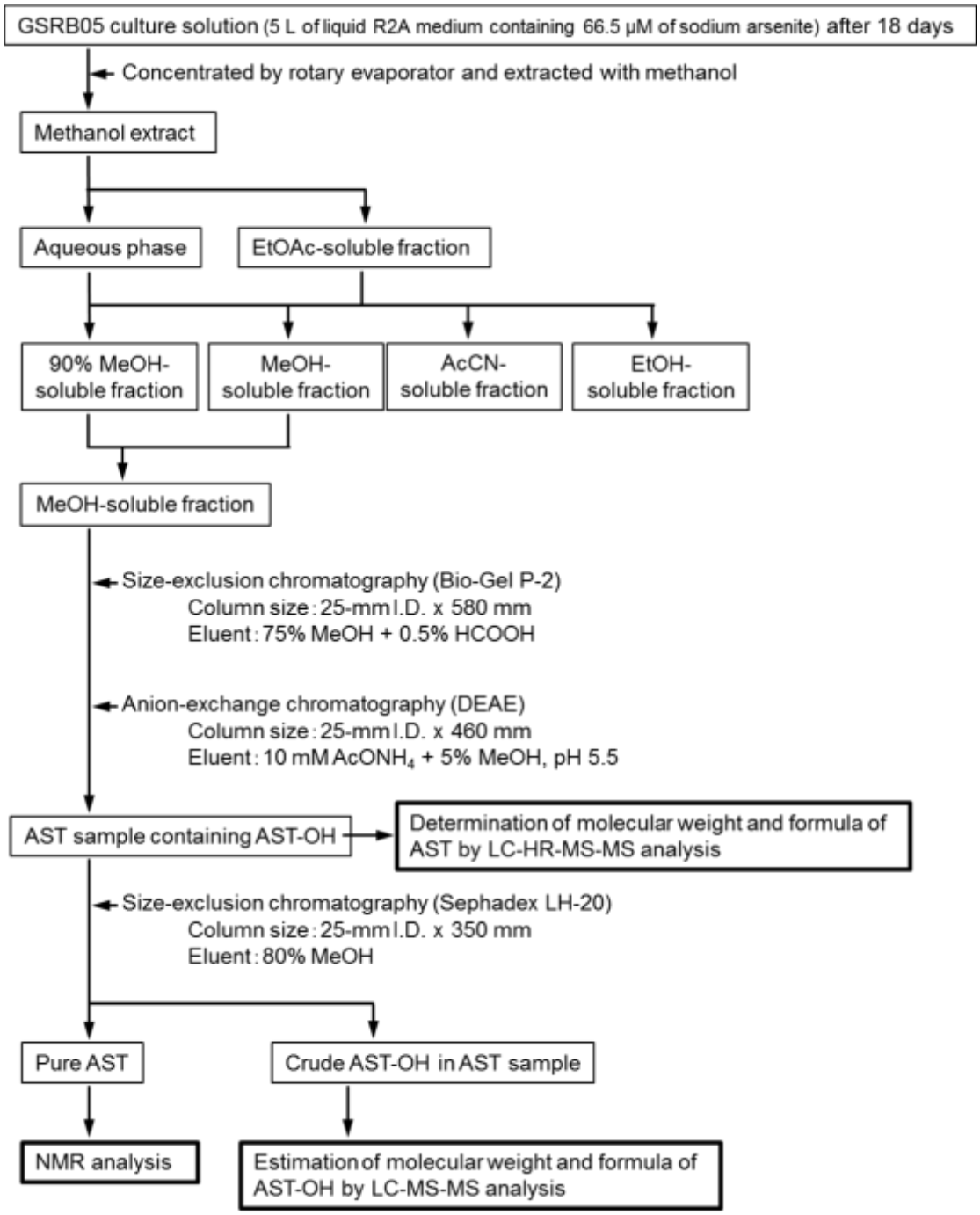

Fig. S1. Purification of arsinothricin (AST) and hydroxyarsinothricin (AST-OH) from the GSRB05 culture medium containing As.

 ©CSIRO 2016

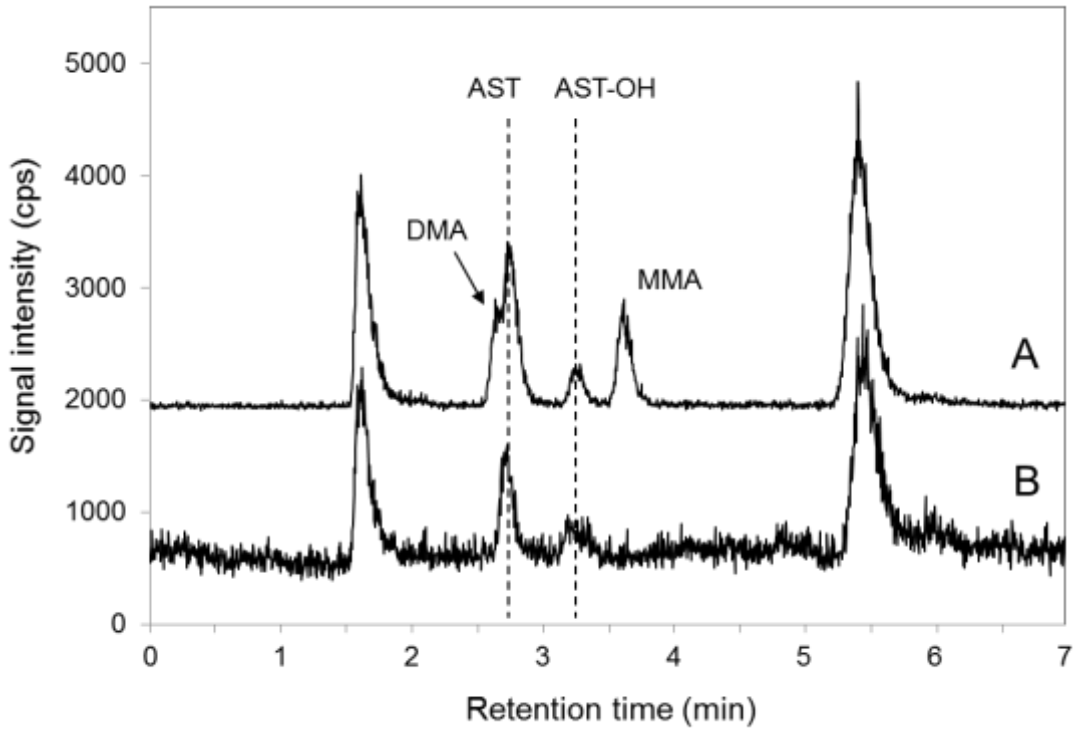

Fig. S2. HPLC-ICP-MS chromatograms of the 120-h sample with DMA and MMA spikes. (a) 2 ng mL^{-1} spikes of DMA and MMA were added to the sample; (b) the original sample. (cps, counts per second.)

 ©CSIRO 2016

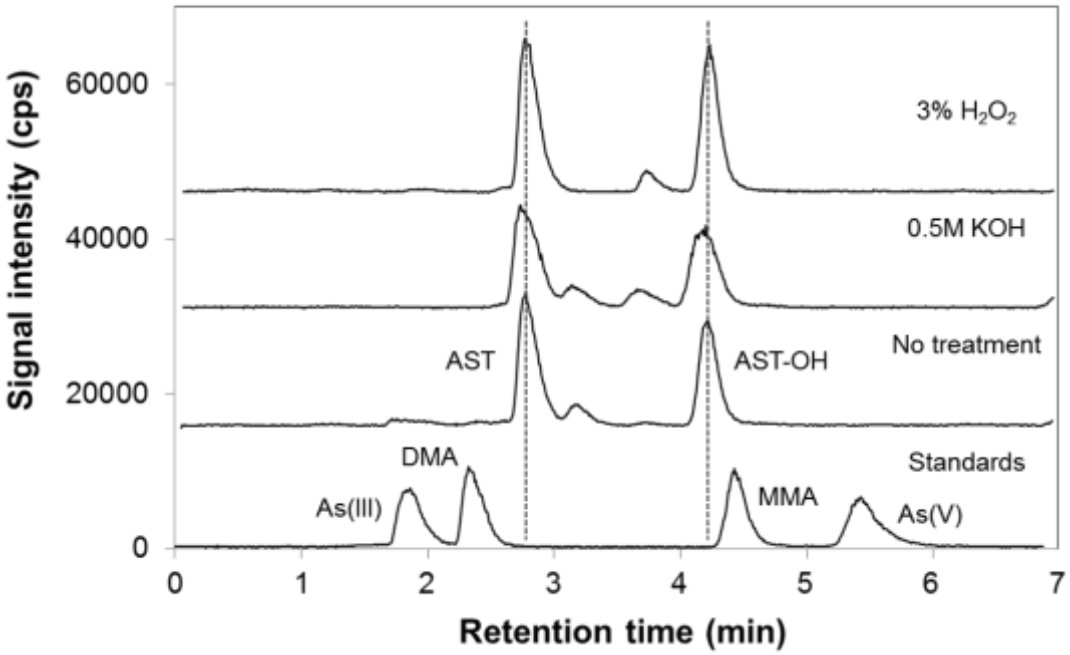

Fig. S3. HPLC-ICP-MS chromatograms of AST and AST-OH after treatment with 3 % H_2O_2 or 0.5 M KOH. (cps, counts per second.)

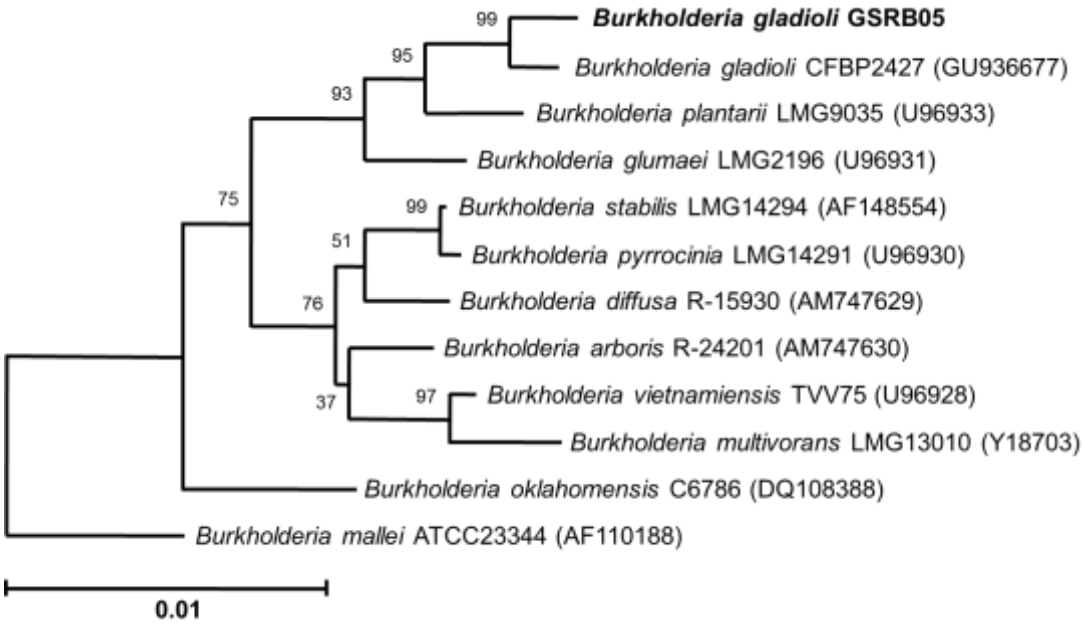

Fig. S4. Phylogenetic relationships of the *Burkholderia gladioli* GSRB05 strain isolated in the present study and related species. The phylogenetic tree of the 16S rRNA sequences was generated by the neighbour-joining method. The tree was tested for support by performing bootstrap resampling (1000 replicates). The bootstrap values are given at each branch; GenBank accession numbers of each sequence employed are in parentheses.

©CSIRO 2016

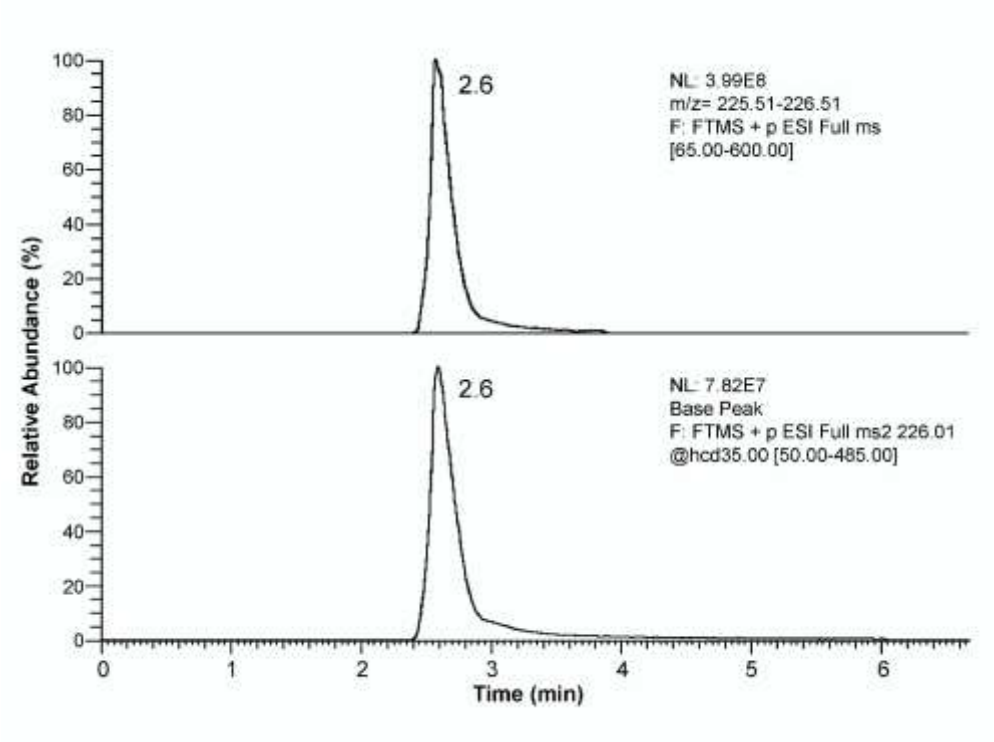

Fig. S5. LC-MS (top) and LC-MS-MS (bottom) chromatograms of AST in the positive-ion mode.

©CSIRO 2016

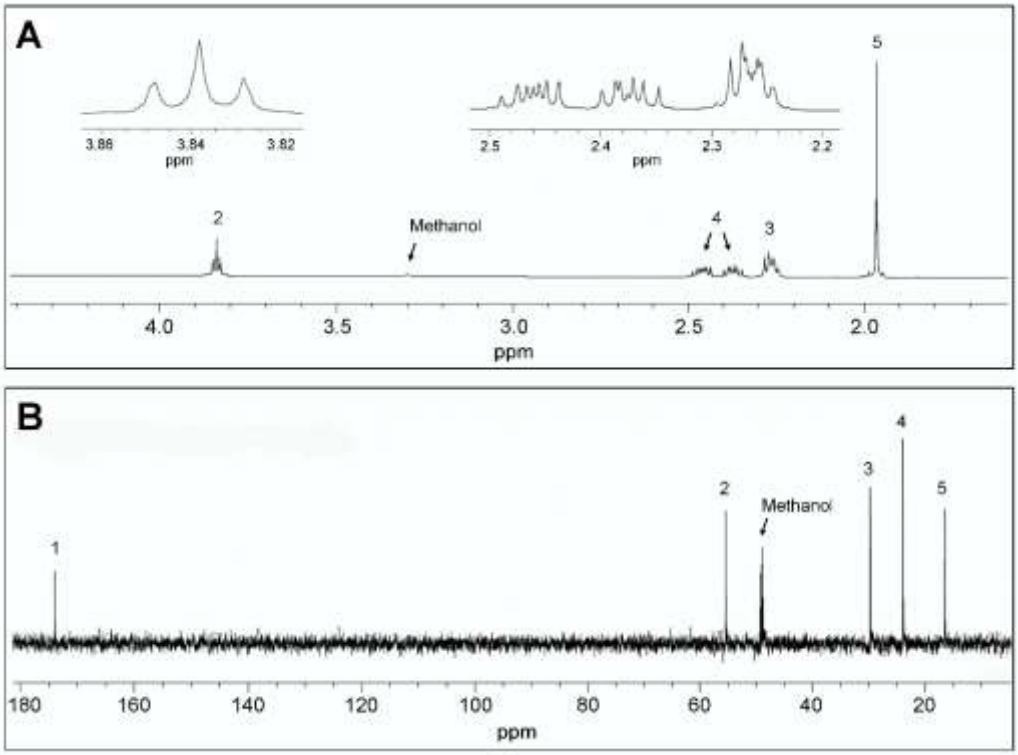

Fig. S6. (a) ^{1}H NMR, and (b) ^{13}C NMR spectra of AST in D_2O. Deuterated methanol (CD_3OD) was added as a chemical shift reference for both NMR analyses.

©CSIRO 2016

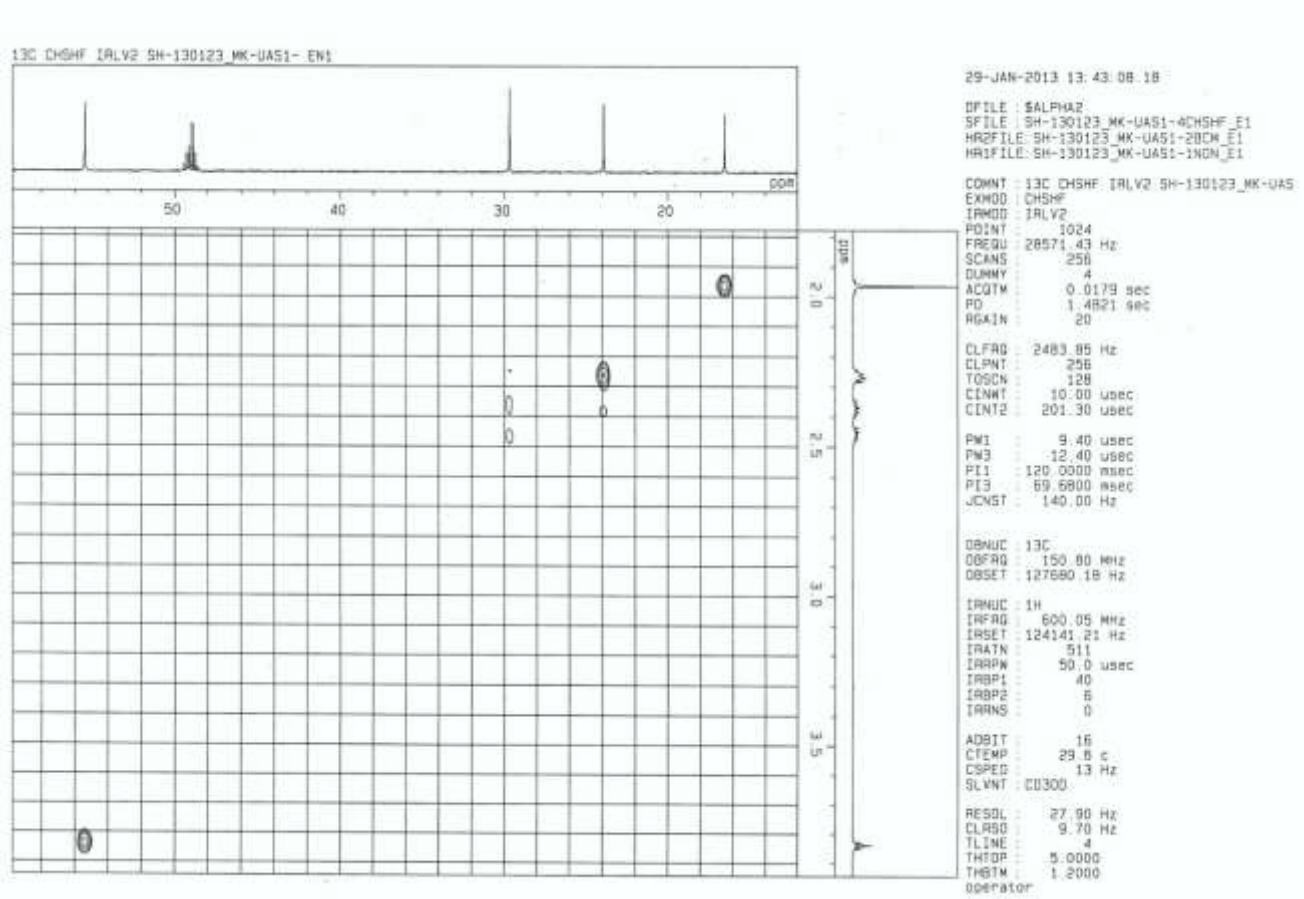

Fig. S7. 2-D HMQC NMR spectrum of AST in D_2O.

©CSIRO 2016

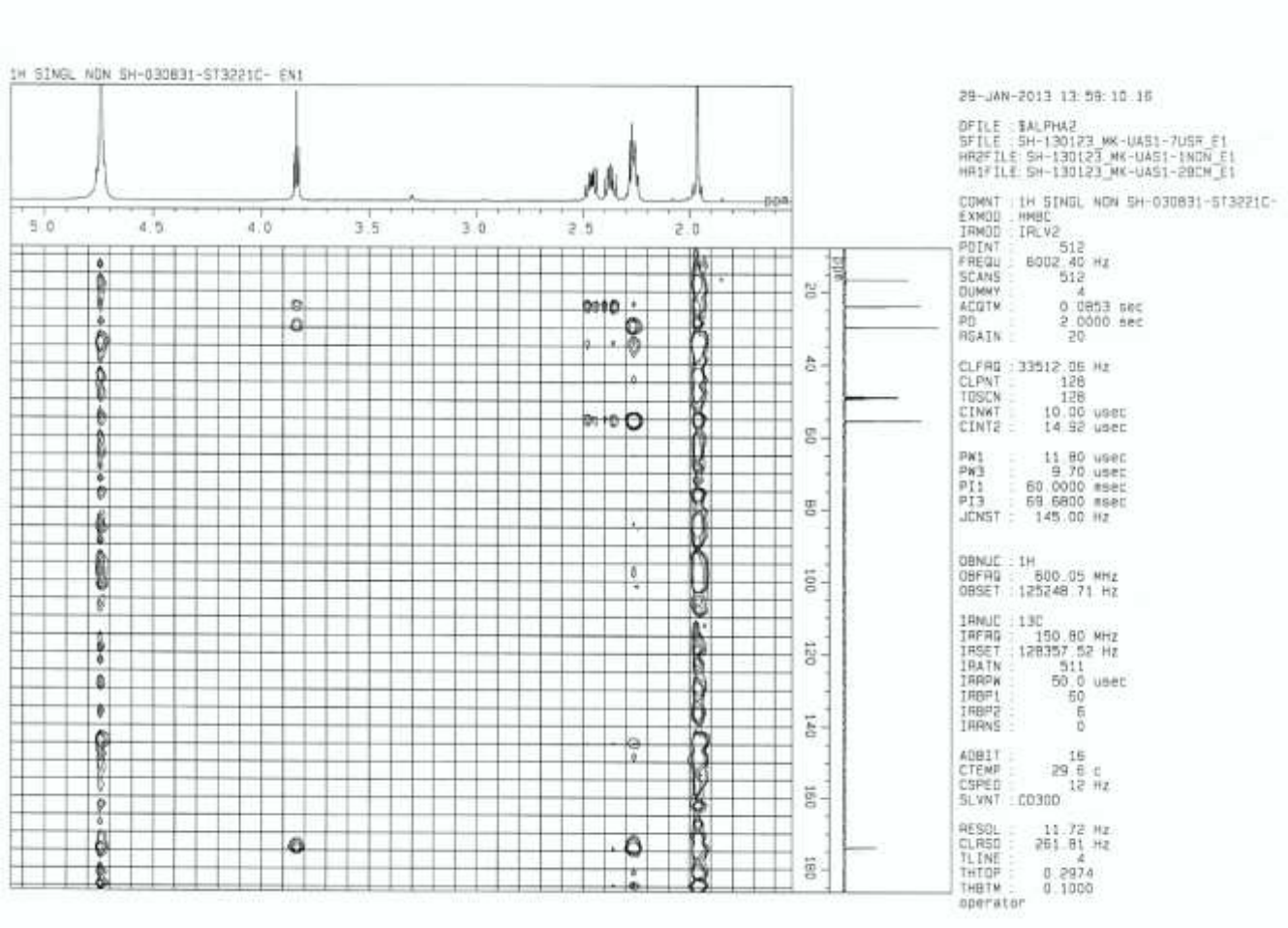

Fig. S8. 2-D ^{1}H–^{1}H COSY NMR spectrum of AST in D_2O.

©CSIRO 2016

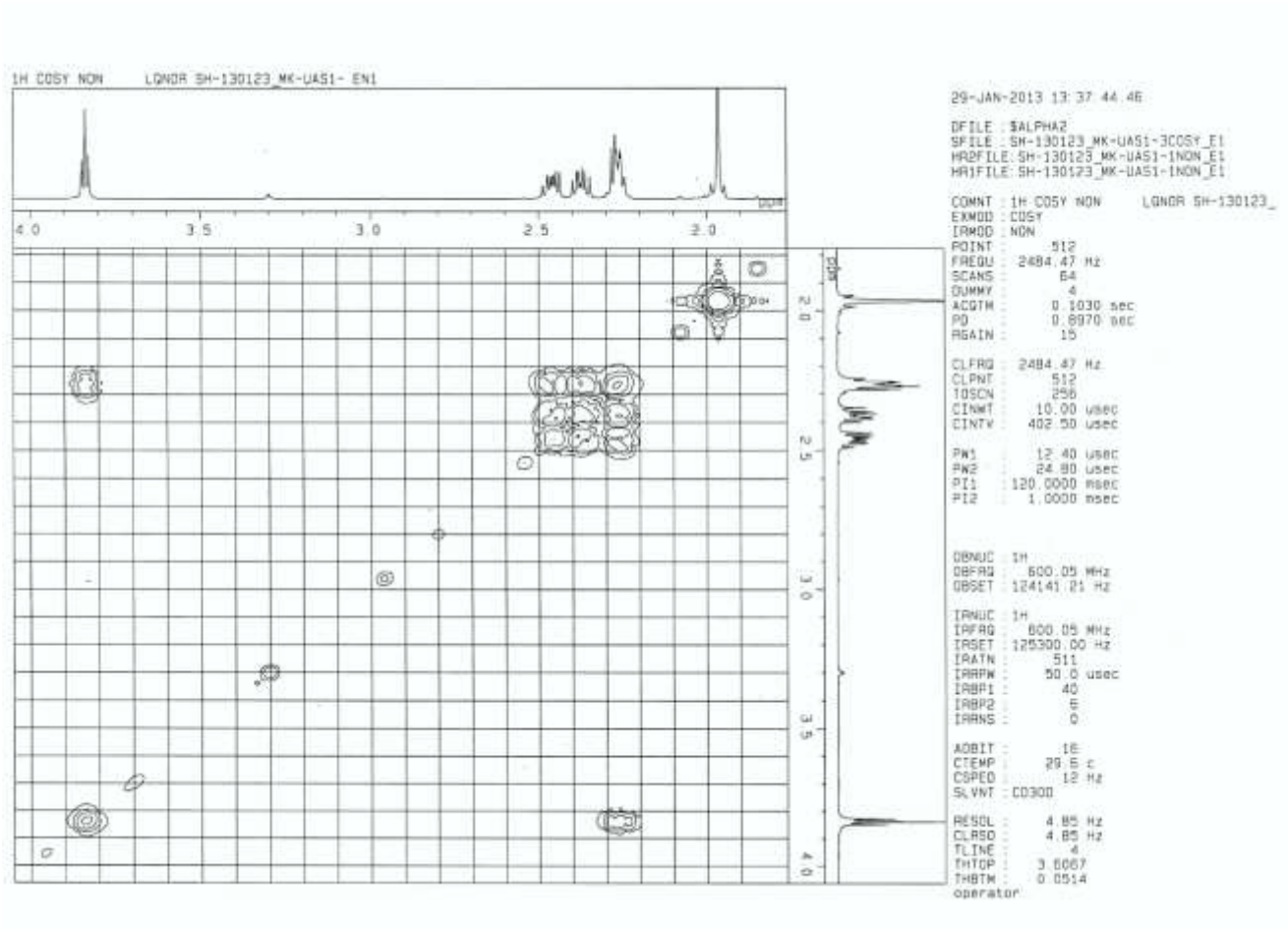

Fig. S9. 2-D HMBC NMR spectrum of AST in D_2O.

 ©CSIRO 2016

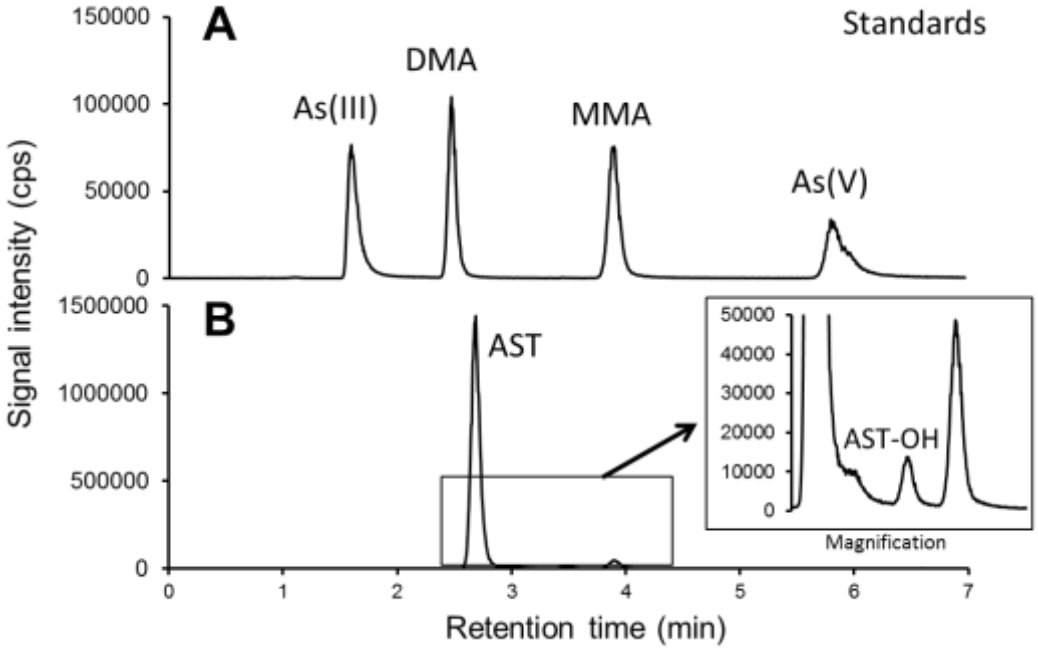

Fig. S10. HPLC-ICP-MS chromatogram of the crude AST sample containing AST-OH. (a) Standard mixture containing As^{III}, As^{V}, MMA and DMA. (b) Crude AST sample containing AST-OH.

 ©CSIRO 2016

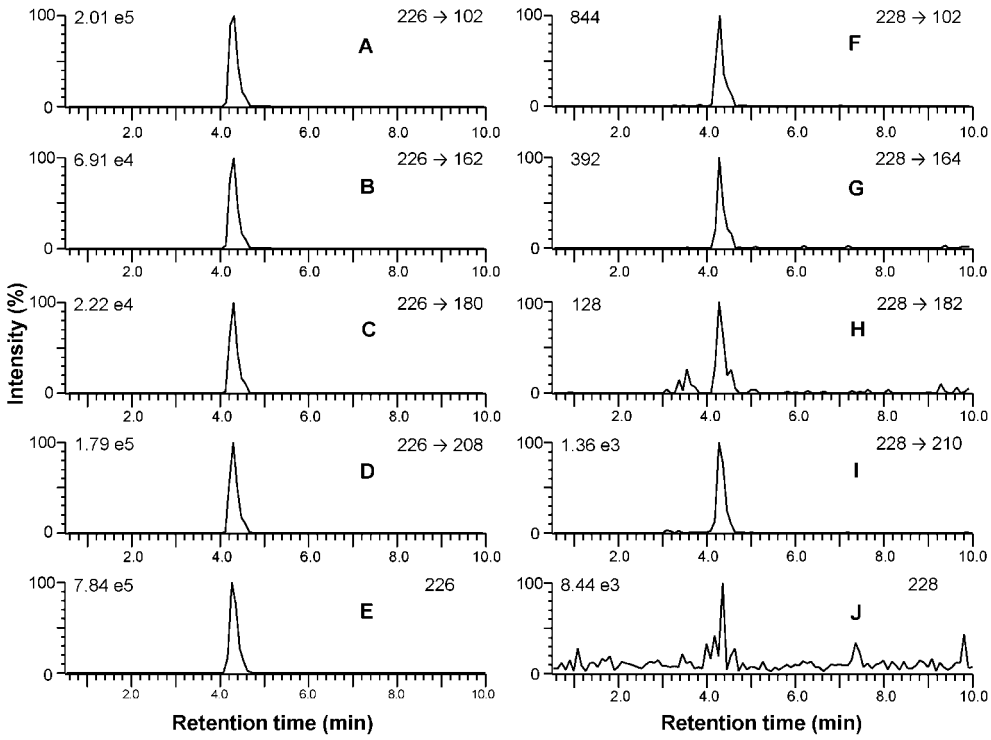

Fig. S11. LC-MS-MS chromatograms for AST and AST-OH at each multiple reaction monitoring (MRM) transition and daughter scan (Fig. S8). Chromatograms A, B, C and D represent the MRM transitions 226 → 102, 226 → 162, 226 → 180 and 226 → 208 respectively; the daughter scan of 226 for AST is shown in E. For AST-OH, chromatograms F, G, H and I represent the MRM transitions 228 → 102, 228 → 164, 228 → 182 and 228 → 210 respectively; the daughter scan of 228 is shown in J.